Received: 11 December 2024 | Revised: 5 March 2025 | Accepted: 5 March 2025

DOI: 10.1002/alz.70141

Alzheimer's & Dementia®
THE JOURNAL OF THE ALZHEIMER'S ASSOCIATION

RESEARCH ARTICLE

The striatum is an early, accurate indicator of amyloid burden using [^{11}C]PiB in Down syndrome: Comparison of two radiotracers

Max McLachlan[1] | Brecca Bettcher[1] | Andrew McVea[1] | Alexandra DiFilippo[1] | Matthew Zammit[1] | Lisette LeMerise[1] | Jeremy Rouanet[2] | Julie Price[3] | Dana Tudorascu[4] | Charles Laymon[4] | David Keator[2] | Patrick Lao[5] | Adam M. Brickman[5] | Tim Fryer[6] | Sigan Hartley[1] | Beau M. Ances[7] | H. Diana Rosas[3] | Sterling Johnson[1] | Tobey Betthauser[1] | Charles K. Stone[1] | Shahid Zaman[6] | Benjamin Handen[4] | Elizabeth Head[2] | Mark Mapstone[2] | Bradley T. Christian[1] | ABC-DS Investigators

[1]School of Medicine and Public Health, University of Wisconsin-Madison, Madison, Wisconsin, USA

[2]School of Medicine, University of California, Irvine, California, USA

[3]Mass General Research Institute, MGH, Harvard Medical School, Boston, Massachusetts, USA

[4]Department of Psychiatry, University of Pittsburgh, Pittsburgh, Pennsylvania, USA

[5]Vagelos College of Physicians and Surgeons, Columbia University, New York, New York, USA

[6]University of Cambridge, The Old Schools, Trinity Ln, Cambridge, TN, UK

[7]Department of Neurology, Washington University in St. Louis, St. Louis, Missouri, USA

Correspondence
Max McLachlan, University of Wisconsin-Madison, 1500 Highland Ave. Rm. T229, Madison, WI 53705, USA.
Email: mclachlan2@wisc.edu

Funding information
DS-Connect (The Down Syndrome Registry); NIH, Grant/Award Numbers: U01 AG051406, U01 AG051412, U19 AG068054, P50 AG008702, P30 AG062421, P50 AG016573, P50 AG005133, P50 AG005681, P30 AG062715, P30 AG066519, P30 AG066468, P30 AG072973, P50 HD105353, U24 AG021886; Eunice Kennedy Shriver National Institute of Child Health and Human Development; National Institute on Aging

Abstract

INTRODUCTION: Adults with Down syndrome demonstrate striatum-first amyloid accumulation with [^{11}C]Pittsburgh Compound-B (PiB) positron emission tomography (PET) imaging, which has not been replicated with [^{18}F]florbetapir (FBP). Early striatal accumulation has not been temporally quantified with respect to global cortical measures.

METHODS: Longitudinal PiB (n = 175 participants) and FBP (n = 92 participants) data from the Alzheimer Biomarkers Consortium-Down Syndrome (ABC-DS) were used to measure cortical and striatal binding. Generalized temporal models for cortical and striatal amyloid accumulation were created using the sampled iterative local approximation (SILA) method.

RESULTS: PiB demonstrated greater striatal-to-cortical ratios than FBP. SILA analysis revealed striatal amyloid burden occurs 3.40 (2.39) years earlier than the cortex in PiB. There was no difference between the cortex and striatum in FBP.

DISCUSSION: Among adults with Down syndrome, the striatum consistently accumulates amyloid earlier than the cortex when measured with PiB. This suggests the striatum is more sensitive to the onset of PiB PET-detectable amyloid in Down syndrome.

KEYWORDS
Alzheimer's disease, Down syndrome, florbetapir, longitudinal, PET imaging, PiB, striatum

Highlights

- Striatal amyloid is detectable 3.4 years before the cortex using PiB PET in DS.
- Florbetapir PET does not detect early striatal amyloid accumulation in DS.
- White matter can be used as reference region in longitudinal florbetapir PET.
- SILA trajectory models can be used to compare regional estimates for age of onset.

1 | INTRODUCTION

Down syndrome (DS) is a developmental disability caused by the triplication of chromosome 21. People with DS carry a 90% lifetime risk of developing Alzheimer's disease (AD),[1] caused by the overproduction of amyloid precursor protein expressed on chromosome 21.[2] Nearly all adults with DS over the age of 40 years exhibit proteinopathies associated with AD, including amyloid plaques and neurofibrillary tau tangles,[3] and the median age for developing clinical symptoms is estimated to be between 50 and 55 years.[4] Consequently, AD is one of the leading causes of death for adults with DS, and the characterization of neuropathological features is necessary to improve long-term health outcomes in this at-risk population.[5]

Amyloid-targeting immunotherapies are emerging treatments for mitigating amyloid plaque accumulation and reducing cognitive impairment associated with late onset AD.[6] Early clinical trials for these therapies excluded individuals with lifelong cognitive dysfunction, such as adults with DS, and limited the age criteria to older cohorts (> 50 or 60 years).[7--9] Additionally, the excess production and accumulation of amyloid (Aβ) in the DS population is associated with significant cerebral amyloid angiopathy (CAA), which is likely to cause complications such as amyloid-related imaging abnormalities (associated with inflammation or stroke).[10] These restrictions prevented the DS population from participating in anti-amyloid drug trials.[11–13] To address these concerns, multiple trial-ready cohorts have recently been established for the DS population,[14,15] and criteria changes have been proposed to the United States Food and Drug Administration (FDA) and drug formularies.[16,17] To provide the same clinical trial opportunities to people with DS and mitigate potential adverse responses, early amyloid detection and accurate disease staging are of critical importance.[18]

The earliest Aβ detection in the DS population is in the striatum based upon studies using positron emission tomography (PET) radiotracer [^{11}C]Pittsburgh Compound-B (PiB). This striatum-first pattern was initially observed with PiB in autosomal-dominant forms of AD (ADAD)[19] – these studies found both greater overall tracer binding in the striatum and earlier binding than the global cortex relative to disease stage.[19–23] This pattern was widely observed across ADAD mutation types, though heterogeneity is observed.[23] Striatum-first accumulation in DS was previously reported in longitudinal studies,[24–26] with detectable accumulation at approximately 40 years of age. These findings are corroborated when DS and ADAD cohorts are compared with sporadic AD.[27,28] When compared longitudinally with the global cortex, the striatum shows significantly earlier accumulation but no difference in the rate of accumulation.[29] Thus, the striatum may serve as an earlier indicator of amyloid burden in the DS population than conventional global cortex measures, such as Centiloids (CLs).[30] However, the extent and magnitude of early striatal amyloid accumulation has not been directly quantified relative to the cortex, limiting its current feasibility for research and clinical use.

The striatum-first pattern of amyloid deposition is exclusively observed using the radiotracer [^{11}C]PiB in both the DS[24–29,31,32] and ADAD[19–23,33] populations. Although striatal binding is consistently reported alongside cortical binding using [^{18}F]florbetapir (FBP) in cross-sectional studies of ADAD and DS,[34–37] striatum-first accumulation has yet to be observed longitudinally or between cognitive groups with this radiotracer.[37–40] For early striatal amyloid accumulation to be a clinically useful measure of AD staging in DS, its prevalence must be confirmed across PET radiotracers used in the DS population.

This study examined longitudinal changes to amyloid PET signal in the striatum using PiB and FBP in DS cohorts. All participants were recruited through the Alzheimer Biomarkers Consortium—Down Syndrome (ABC-DS), a large multi-site study investigating AD-related pathology in adults with DS.[14] To produce general models for the longitudinal change of Aβ PET in these regions, the sampled iterative local approximation (SILA) algorithm was implemented. SILA is used to combine large longitudinal amyloid PET datasets in both the late onset AD and DS populations.[41,42] SILA's estimates for age-of-pathology-onset are particularly useful for staging AD pathologies temporally. In this study, the SILA method was applied to both cortical and striatal PET data, allowing for the direct comparison of the estimated age-of-onset in each region.

2 | METHODS

2.1 | Participants

At four ABC-DS sites, 175 participants (47.4% female; average age at baseline visit = 37.1 (8.0) years) underwent up to six PiB PET imaging scans. At three ABC-DS sites, a separate group of 97 participants (35.9% female; average age at baseline visit = 50.1 (7.2) years) underwent up to four FBP PET imaging scans. Time between longitudinal PiB scans was approximately 3.2 (0.9) years, while time between longitudinal FBP scans was approximately 1.6 (0.8) years. All participants received structural T1-weighted imaging at each timepoint. Blood samples were collected at each timepoint to determine apolipoprotein E (APOE) allele status. A case consensus conference determined cognitive status, as described previously.[28] The study was approved by an Institutional Review Board and conducted in accordance with the Declaration of Helsinki. Informed consent and assent were obtained prior to conducting any study activities. The enrollment criteria for PiB sites included being ≥ 25 years of age and having a nonverbal mental age of at least 3 years, based on the Stanford-Binet, 5th edition. The enrollment criteria for the FBP sites included being ≥ 40 years of age, resulting in an older cohort relative to the PiB cohort. All participants received genetic testing to confirm DS status by karyotype. Exclusion criteria restricted those having an unstable psychiatric or medical condition that impaired cognition or contraindicated the acquisition of brain imaging scans. Note that the distinct age enrollment criteria resulted in different age and cognitive status distributions across the two radiotracer cohorts. During enrollment, this multi-site study aimed to include participants from broad racial, ethnic, socioeconomic, and geographic backgrounds to ensure representation consistent with the DS population in the general public. See Table 1 for information about longitudinal scanning and participant demographics.

2.2 | MR imaging

T1-weighted magnetic resonance images (MRIs) were acquired on the following scanners, depending on the imaging site: 3T GE Discovery MR750, Siemens MAGNETOM Prisma^{Fit}, GE Signa PET/MR, Siemens Biograph mMR, and Phillips Achieva. T1-weighted scans were acquired with one of the following sequences: 3D fast spoiled gradient echo (FSPGR) or magnetization-prepared rapid gradient-echo (MP-RAGE). Images were corrected for magnetic field bias and gradient nonlinearity, and a quality control procedure evaluated images for any remaining artifacts.

2.3 | PET imaging

PiB PET scans (target injected dose of 15 mCi) were acquired on the following scanners, depending on the imaging site: ECAT EXACT HR+, SIGNA PET/MR, Biograph 64 mCT, Discovery 710, Biograph 40 True Point. FBP PET scans (target injected dose of 10 mCi) were acquired on the following scanners, depending on the imaging site: HRRT, Biograph 64 mCT, Biograph mMR, Biograph 64 mCT 4R. PET data were collected 50–70 min post-intravenous injection for both PiB and FBP, resulting in four 5-min frames for each scan.

RESEARCH IN CONTEXT

1. **Systematic review**: The authors reviewed available literature using traditional public sources (e.g. PubMed), meeting abstracts, and meeting presentations. Striatal accumulation has been observed previously using [^{11}C]Pittsburgh Compound-B (PiB) positron emission tomography (PET) in Down syndrome and autosomal dominant Alzheimer's disease cohorts. These papers were cited appropriately.
2. **Interpretation**: Our findings provide an estimate for the temporal relationship between amyloid detectability in the striatum relative to the global cortex using PiB. Additionally, we report that imaging with florbetapir does not reflect the same relationship.
3. **Future directions**: The findings in this manuscript encourage further investigations into striatal accumulation in Down syndrome cohorts using alternative amyloid radiotracers. Specifically, our work encourages future studies on (1) the pathology of amyloid plaque in the striatum of people with Down syndrome and (2) the binding affinities for amyloid plaque subtypes of PiB, florbetapir, and other modern amyloid tracers.

2.4 | Image processing

All image post-processing was performed using statistical parametric mapping software (SPM12). Individual T1-weighted MRIs underwent tissue classification using SPM12 Segmentation. The brain was skull-stripped by combining the white matter (WM), gray matter (GM), and cerebrospinal fluid (CSF) tissue segmentations as follows: WM + GM + 0.25*CSF (CSF is included to improve spatial normalization to ventricles and other low intensity regions in the MRI). An eroded WM (EWM) mask was produced from each magnetic resonance imaging (MRI) scan by smoothing the WM segmentation to 8 mm resolution and thresholding to 90% tissue probability. This produced participant-specific masks containing the centrum semiovale, pons, cerebellar WM, and corpus callosum.

PET images were smoothed to 8 mm isotropic resolution, accounting for PET scanner resolution and site-specific smoothing. Images were summed 50–70 min and co-registered to the participant's T1-weighted MRI using SPM12 Coregister. The skull-stripped MRI was normalized to a DS-specific template MRI (LeMerise et al; AAPM 2022) using the SPM12 Old Normalize function. The same transformation

TABLE 1 Participant demographics for PiB (top) and FBP (bottom) cohorts.

	No. of scans [*n*]				
Parameter	**1 Scan**	**2 Scans**	**3 Scans**	**≥4 Scans**	**All participants**
PiB					
Cohort size [*n*]	64	59	15	37	175
Age at baseline, mean (SD) [yr]	39.5 (SD = 9.1)	35.0 (SD = 7.4)	37.4 (SD = 6.9)	36.0 (SD = 6.4)	37.1 (SD = 8.0)
Female [n (%)]	28 (43.8)	32 (54.2)	6 (40.0)	17 (46.0)	83 (47.4)
APOE e4 carrier [*n* (%)]	13 (20.6)	17 (28.8)	3 (20.0)	4 (10.8)	37 (21.3)
Aβ Status					
Aβ- [n (%)]	46 (71.9)	45 (76.3)	6 (40.0)	16 (43.2)	113 (64.6)
Aβ Converter [n (%)]	N/A	7 (11.9)	5 (33.3)	17 (45.9)	29 (16.6)
Aβ+ [n (%)]	18 (28.1)	7 (11.9)	4 (26.7)	4 (10.8)	33 (18.9)
Cognitive status					
CS [n (%)]	54 (84.4)	54 (91.5)	9 (60.0)	27 (73.0)	144 (82.3)
MCI [n (%)]	1 (1.6)	1 (1.7)	1 (6.7)	4 (10.8)	7 (4.0)
Dementia [n (%)]	4 (6.3)	4 (6.8)	4 (26.7)	6 (16.2)	18 (10.3)
Undetermined [n (%)]	5 (7.8)	0 (0.0)	1 (6.7)	0 (0.0)	6 (3.4)
Hispanic [n (%)]	3 (4.7)	1 (1.7)	0 (0.0)	0 (0.0)	4 (2.3)
Race					
White [n (%)]	61 (95.3)	59 (100.0)	14 (93.3)	37 (100.0)	171 (97.7)
Black/African-American/ African/Caribbean/Black British [n (%)]	2 (3.1)	0 (0.0)	0 (0.0)	0 (0.0)	2 (1.1)
American Indian/ Alaskan Native [n (%)]	0 (0.0)	0 (0.0)	1 (6.7)	0 (0.0)	1 (0.6)
Asian/Asian British [n (%)]	1 (1.6)	0 (0.0)	0 (0.0)	0 (0.0)	1 (0.6)
Native Hawaiian/Other Pacific Islander [n (%)]	0 (0.0)	0 (0.0)	0 (0.0)	0 (0.0)	0 (0.0)
FBP					
Cohort size [n]	25	29	29	9	92
Age at baseline, mean (SD) [yr]	52.8 (SD = 7.6)	49.1 (SD = 7.4)	49.3 (SD = 6.6)	48.7 (SD = 6.7)	50.1 (SD = 7.2)
Female [*n* (%)]	11 (44.0)	12 (41.4)	7 (24.1)	3 (33.3)	33 (35.9)
APOE e4 carrier [*n* (%)]	5 (20.0)	6 (20.7)	7 (24.1)	3 (33.3)	21 (22.8)
Aβ Status					
Aβ- [n (%)]	7 (28.0)	4 (13.8)	4 (13.8)	1 (11.1)	16 (17.4)
Aβ Converter [n (%)]	N/A	0 (0.0)	6 (20.7)	2 (22.2)	8 (8.7)
Aβ+ [n (%)]	18 (72.0)	25 (86.2)	19 (65.5)	6 (66.7)	68 (73.9)
Cognitive status					
CS [n (%)]	9 (36.0)	10 (34.5)	13 (44.8)	6 (66.7)	38 (41.3)
MCI [n (%)]	2 (8.0)	9 (31.0)	7 (24.1)	2 (22.2)	20 (21.7)
Dementia [n (%)]	14 (56.0)	10 (34.5)	9 (31.0)	1 (11.1)	34 (37.0)
Undetermined [n (%)]	0 (0.0)	0 (0.0)	0 (0.0)	0 (0.0)	0 (0.0)
Hispanic [n (%)]	1 (4.0)	2 (6.9)	2 (6.9)	3 (33.3)	8 (8.7)
Race					
White [n (%)]	25 (100.0)	27 (93.1)	28 (96.6)	8 (88.9)	88 (95.7)
Black/African-American/ African/Caribbean/ Black British [n (%)]	0 (0.0)	0 (0.0)	1 (3.4)	0 (0.0)	1 (1.1)
American Indian/ Alaskan Native [n (%)]	0 (0.0)	0 (0.0)	0 (0.0)	0 (0.0)	0 (0.0)
Asian/Asian British [n (%)]	0 (0.0)	2 (6.9)	0 (0.0)	1 (11.1)	3 (3.3)
Native Hawaiian/Other Pacific Islander [n (%)]	0 (0.0)	0 (0.0)	0 (0.0)	0 (0.0)	0 (0.0)

Note: Amyloid positivity was determined using a cutoff of 18.1 Centiloids (CL). Aβ converters have at least one Aβ- scan followed by an Aβ+ scan.
Abbreviations: Aβ, beta amyloid; APOE, apolipoprotein E; CS, cognitively stable; FBP, [^{18}F]florbetapir; MCI, mild cognitive impairment; PiB, Pittsburgh Compound-B.

matrix was applied to the co-registered PET scan to warp them into a common imaging space.

Global amyloid burden was calculated following the CL calibration procedure.[30] The CL global cortical region of interest (ROI), whole cerebellum (WC) ROI, and the Harvard Oxford Atlas were warped into the DS template space using SPM12 Old Normalize. The warped ROIs were smoothed by 2 mm to improve margin uniformity. For PiB, standardized uptake value ratio 50-70 ($SUVR_{50\text{-}70}$) parametric images were created using the WC as reference region.[43] For FBP, the WC and WM regions are used as reference regions in the NT population—most studies report the greatest power and longitudinal stability when using WM-based reference regions.[44,45] To determine the optimal reference region for longitudinal comparison in the DS population, $SUVR_{50\text{-}70}$ parametric images were created for each FBP scan using both the WC and participant-specific EWM as reference regions. Stability of longitudinal trajectories determined which reference region was used for the remaining analyses in all FBP scans. A CL calibration was then performed for both the PiB and FBP processing methods.[30]

Average cortical SUVR was converted to CL. Participants were initially grouped by amyloid positivity status using the published threshold of 18.1 CL.[24] An average PET image was created for each group. A PET-generated striatum ROI was then created by subtracting the average Aβ- PiB image from the average Aβ+ PiB image, thresholding to a difference of +0.75 SUVR units, and removing unassociated regions. SUVR was calculated for the caudate, putamen, accumbens, composite MRI-based striatum (all made using the Harvard Oxford Atlas), and the PET-generated striatum.

2.5 | Statistics

For the FBP reference region analysis, the average rate of cortical SUVR change was assessed with % change/year = ($SUVR_2$-$SUVR_1$)/($SUVR_1$*Δt). The number of scans with positive longitudinal changes was counted for each reference region. SUVR was assessed using a linear mixed effects (LME) model of the form SUVR ~ Scanner (four different scanners) + Time (relative to first scan) + Reference Region, with a random participant-level intercept. A paired *t*-test and Levene's test evaluated differences in the distributions of % change/year for each reference region method. Group differences in WM-to-cerebellum uptake ratios were also evaluated between PiB and FBP groups.

For each PET scan, the striatum-to-cortex uptake ratio was calculated. To minimize group-level differences in Aβ status, scans were CL matched within ± 5 CL across tracers. Only one scan per participant was permitted to be matched. The data from the matched participants were incorporated into a linear model of the form Ratio ~ CL + CL^2 + Tracer + Sex + Age + Cognitive Status (Non-CS) + APOE4 + Race (Non-White) + Ethnicity (Hispanic). Interaction terms between Tracer and other covariates were also investigated. Significance of model terms was evaluated using Type 2 analysis of variance (ANOVA). Effect size was calculated using Cohen's f statistic for each model term.

Positivity thresholds were calculated for all striatum-specific ROIs and the cortical ROI (for consistency) using a gaussian mixture model with two distributions. The thresholds were defined as $\bar{x}_{lower} + 2 * SD_{lower}$.[46] Following the SILA method, the average rate of change was calculated within discrete SUVR intervals. Defining $t = 0$ as the time of positivity, Euler's method determines the average longitudinal change. This process yields generalized models for the progression of SUVR relative to positivity in each ROI. The estimated time-to-amyloid-positivity for each participant and ROI was calculated by minimizing the sum of squared differences between participant trajectories and the models. Paired *t*-tests evaluated the average differences in time-to-positivity between the cortex and each striatum-specific ROI. Estimates from SILA are most reliable for trajectories that have crossed the positivity threshold; therefore, this analysis was only performed for participants with at least one positive scan in each ROI. Additionally, SILA estimates were only compared within-tracer to avoid bias in the difference calculation.

Each SILA model is plotted relative to the individual ROI's time-to-positivity axis, meaning the models do not inherently exist on the same time axis. In order to compare the striatum model to the cortex model, the cortex model was shifted by the average time difference found from the paired *t*-tests. Following this transformation, the striatum-to-cortex model ratio can be calculated.

3 | RESULTS

3.1 | FBP reference region comparison

Figure 1 displays FBP cortical longitudinal trajectories and % change/year between timepoints using WC and EWM reference regions. With the WC reference region, 67/114 (59%) consecutive scans show longitudinal increases in amyloid, with the average rate of change being 1.92 ± 6.04%/year. With the EWM reference region, 94/114 (82%) consecutive scans show longitudinal increases, with the average rate of change being 1.98 ± 2.97%/year. Based on the LME model, $SUVR_{EWM}$ is lower than $SUVR_{WC}$ ($p < 0.001^{***}$). All model estimates are provided in Supplementary Material. A paired *t*-test for % change/year showed no significant difference between the means of the reference region methods ($p = 0.909$). Levene's test showed a significant reduction in variance when using the EWM reference region, with an estimated variance ratio $\sigma^2_{EWM}/\sigma^2_{WC} = 0.259$ [0.167,0.351] ($p < 0.001^{***}$). As the EWM reference region method showed a greater number of participants with longitudinal increases and lower group variance, $SUVR_{EWM}$ was used for the remaining analysis with all FBP scans. A CL calibration is included in Supplementary Material for both PiB and FBP.

3.2 | PiB/FBP comparison

Figure 2 displays longitudinal trajectories for PiB and FBP in both the cortex and PET-generated striatum ROIs. Figure 3 shows

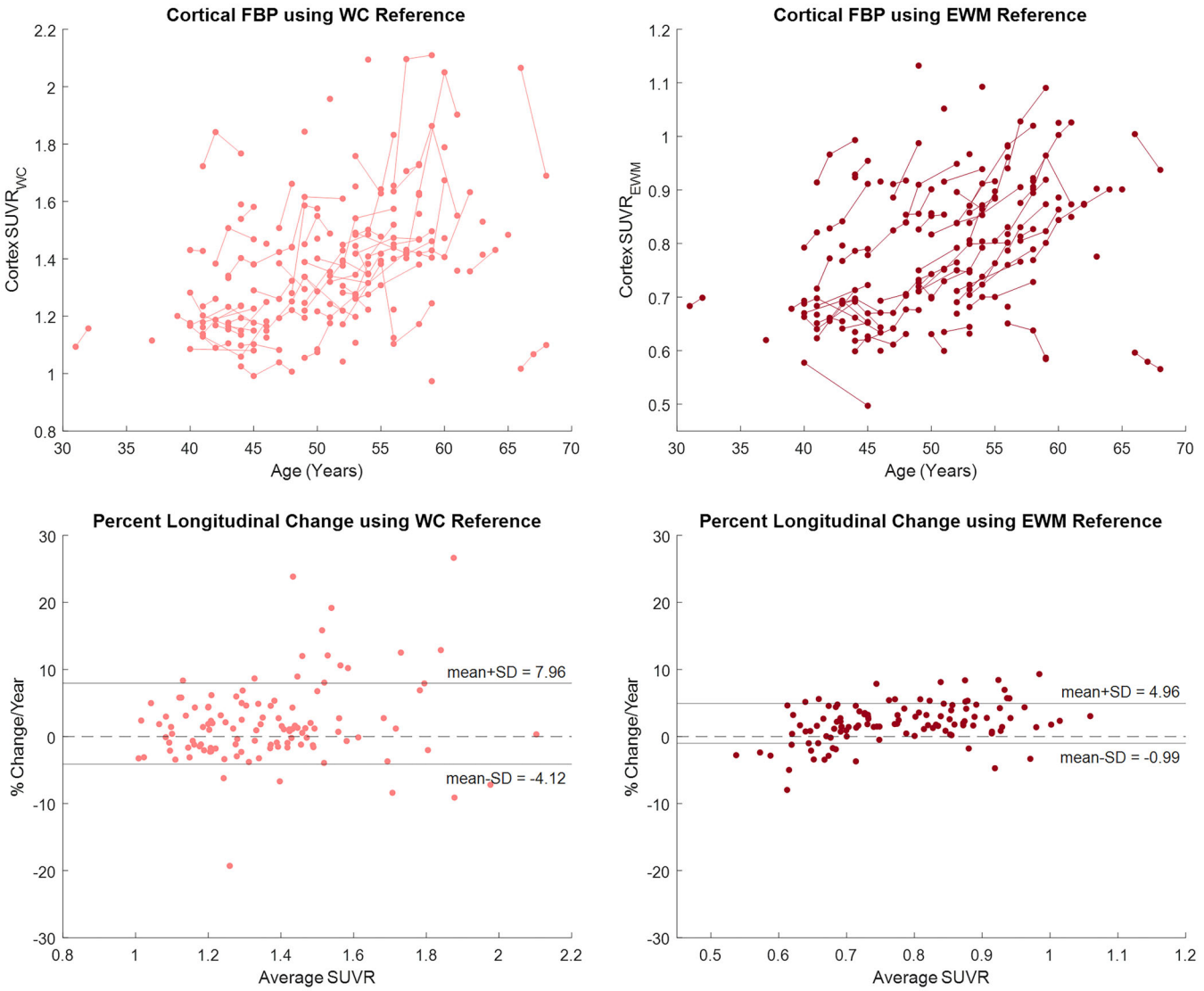

FIGURE 1 Longitudinal FBP trajectories (top) and percent longitudinal change (bottom) using EWM and WC reference regions, showing that using EWM provides more sensitivity and less variability. Light marker colors correspond to WC-based processing, and dark marker colors correspond to EWM-based processing. $SUVR_{EWM}$ has a lower and compressed range when compared to $SUVR_{WC}$. Percent longitudinal change was calculated as follows: % change/year = $(SUVR_2\text{-}SUVR_1)/(SUVR_1{}^{*}\Delta t)$. EWM, eroded white matter; FBP, [^{18}F]florbetapir; SUVR, standardized uptake value ratio; WC, whole cerebellum.

average Aβ- and Aβ+ images for each radiotracer, as well as % difference images between amyloid groups. Both tracers demonstrated the highest change in amyloid in cortical regions, particularly the precuneus and striatum. PiB showed greater overall range of % difference, likely influenced by the greater dynamic range of $SUVR_{WC}$ compared to $SUVR_{EWM}$.

CL matching across tracers resulted in 66 matched pairs (demographics in Supplementary Materials). The groups showed significant sex and age differences. These scans were used for the linear model Ratio ~ CL + CL^2 + Tracer + Sex + Age + Cognitive Status (Non-CS) + APOE4 + Race (Non-White) + Ethnicity (Hispanic) (Figure 4). Participants who were imaged with PiB show a significantly higher striatum-to-cortex ratio than those imaged with FBP ($p < 0.001^{***}$), with the modeled ratio maximizing at approximately 75 CL. The Tracer model term has the largest effect size, followed by CL terms and APOE4 status (Table 2). The Tracer:APOE4 interaction term was significant and retained in the model.

Across the entire cohort, PiB had higher SUVR in the striatum than the cortex, with an average difference of 0.13 SUVR (two-sample *t*-test, Cohen's $d = 0.35$, $p < 0.001^{***}$). FBP showed an average difference between striatum SUVR and cortex SUVR of 0.01 (two-sample *t*-test, Cohen's $d = 0.04$, $p = 0.155$). Additionally, FBP showed a significantly higher WM-to-cerebellum ratio on average (1.76 (0.14)) compared to PiB (1.63 (0.11)) across the entirety of both cohorts (two-sample *t*-test, Cohen's $d = 1.05$; $p < 0.001^{***}$).

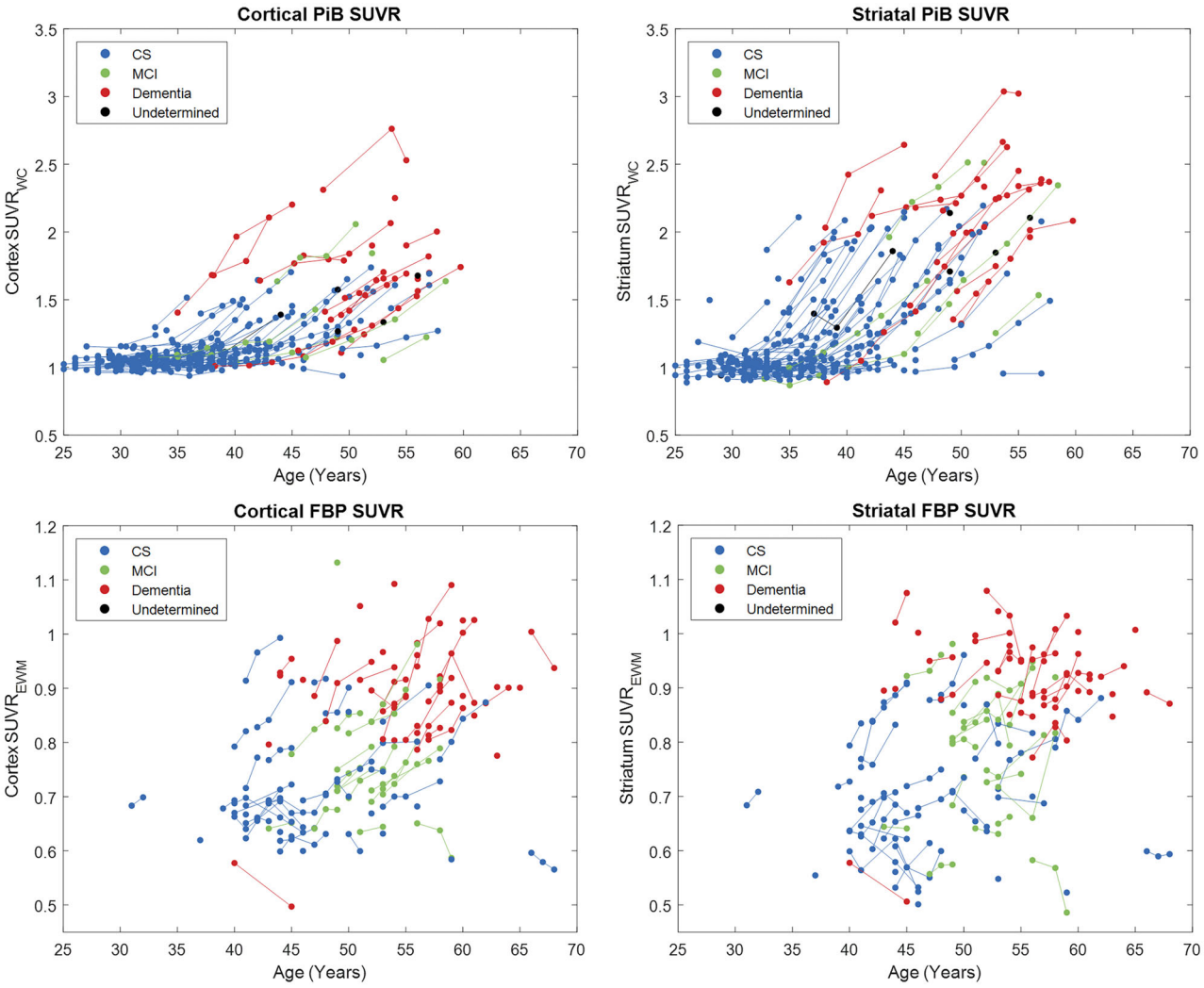

FIGURE 2 Longitudinal PiB (top) and FBP (bottom) trajectories for both the global cortex and PET-generated striatum ROI. Cognitive status is denoted by marker color. FBP, [^{18}F]florbetapir; PET, positron emission tomography; PiB, Pittsburgh Compound-B; ROI, region of interest.

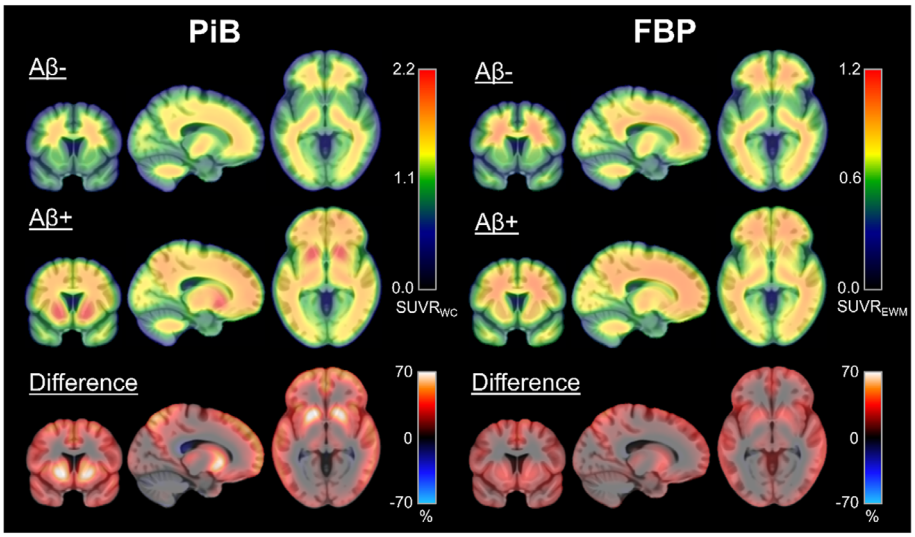

FIGURE 3 Average PET SUVR images by amyloid status. Percent difference image shows the greatest PET signal in the precuneus and striatum for both tracers, though PiB has a greater dynamic range and shows much higher relative signal than FBP. PET, positron emission tomography; PiB, Pittsburgh Compound-B; SUVR, standardized uptake value ratio.

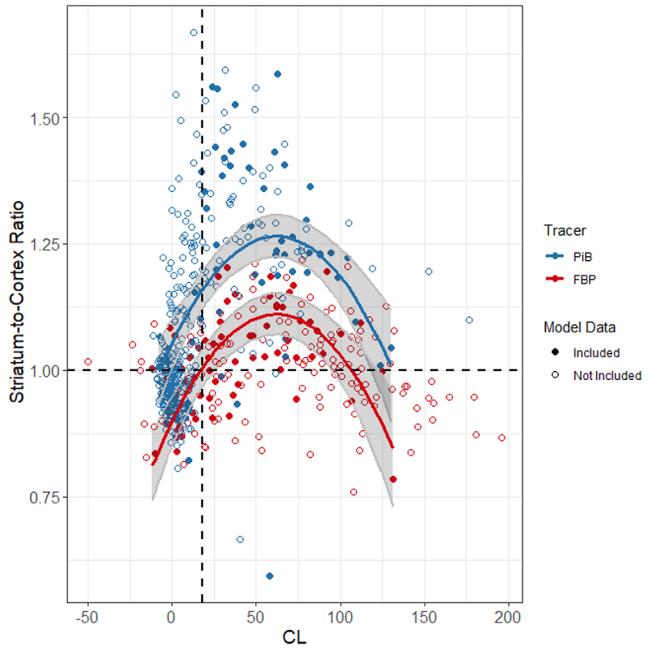

FIGURE 4 Multivariate linear model for the striatum-to-cortex ratio. CL-matched scans (included in the model) are denoted by solid markers. For visual simplicity, the displayed model is of the form Ratio ~ CL + CL^2 + Tracer. CL, Centiloid.

TABLE 2 Parameter estimates and significance for multivariate linear model.

Model term	*β* [95% CI]	*p*-Value	Cohen's f
Intercept	0.767 [0.605, 0.928]	N/A	N/A
CL	5.206e-3 [3.088e-3, 7.324e-3]	<0.001***	0.44 (L)
CL^2	−4.520e-5 [−6.321e-5, −2.719e-5]	<0.001***	0.45 (L)
Tracer	**0.209 [0.155, 0.263]**	**<0.001*** **	**0.65 (L)**
Sex	3.612e-2 [−1.133e-2, 8.357e-2]	0.134	0.14 (S)
Age	2.645e-3 [1.002e-3, 6.291e-3]	0.154	0.13 (S)
Cognitive status (Non-CS)	2.501e-2 [−3.342e-2, 8.344e-2]	0.398	0.08
APOE4	8.160e-3 [−6.910e-2, 8.542e-2]	0.023*	0.21 (S)
Race (Non-White)	5.864e-2 [−7.361e-2, 0.191]	0.382	0.08
Ethnicity (Hispanic)	−2.392e-3 [−1.126e-1, 1.078e-1]	0.966	0.00
Tracer:APOE4	−0.151 [−0.262, −4.039e-2]	0.008**	0.24 (S)

Note: For Cohen's *f*: $f = 0.10$ is the suggested cutoff for a small effect size (S). $f = 0.25$ is the suggested cutoff for a medium effect size (M). $f = 0.40$ is the suggested cutoff for a large effect size (L).
Abbreviations: APOE, apolipoprotein E; CI, confidence interval; CL, Centiloid; CS, cognitively stable.

3.3 | SILA analysis

SILA modeling was completed on the cortex and all striatum-specific regions using GMM-derived cutoffs (listed in Supplementary Materials). In general, all A*β*-converting participants have a striatum positive timepoint before their first cortex positive timepoint in the PiB cohort. For each participant with at least one positive scan, the estimated time-to-cortex-positivity was subtracted from the estimated time-to-positivity in each striatum-specific region (Figure 5). For PiB, the PET-based striatum showed the earliest positivity estimates, on average 3.40 (2.39) years before the cortex. The caudate showed the latest positivity estimates, on average 4.22 (10.98) years after the cortex. Other than the caudate, all striatum ROIs showed earlier time-to-positivity estimates than the cortex in the PiB cohort. For FBP, the PET-based striatum, putamen, and accumbens ROIs did not show different time-to-positivity estimates than the cortex. SILA models could not be generated for the caudate and MRI-based striatum ROIs, as high longitudinal variability in these regions resulted in a nonmonotonic model.

To determine the striatal-to-cortical ratio relative to time-to-positivity in PiB, the cortical SILA curve was shifted by the average calculated difference (3.40 years), aligning the model on the PET-based striatum positivity axis (Figure 6). At the time of striatum positivity, the ratio of the two SILA models (striatum-to-cortex ratio) was 1.03 [1.01, 1.06]. At the time of cortical positivity, the ratio of the two SILA models was 1.16 [1.13,1.20].

4 | DISCUSSION

With the development and implementation of anti-amyloid therapies, early detection of AD pathology is critical for identifying appropriate inclusion of people with DS in clinical trials.[18] This study supports previous findings that the striatum is the earliest region of amyloid accumulation detectable using [^{11}C]PiB in people with DS. Furthermore, FBP is insensitive to striatum-first accumulation in DS, suggesting there exists a fundamental difference in the binding targets or affinities between PiB and FBP in the striatum.

The exact mechanism through which PiB detects early striatal accumulation is unknown. *Post mortem* histopathological studies demonstrated the presence of diffuse A*β* plaque in the striatum for both ADAD[47–49] and DS.[50–52] These diffuse plaques are largely formed from A*β*42 peptides rather than A*β*40.[48,53] High binding affinity for A*β*42 neuritic plaques is well documented for both PiB[54,55] and FBP.[56,57] Binding to diffuse plaque is less understood, which likely contributes to discrepancies observed between *post mortem* pathology and in vivo PET measures.[58] Neuropathology studies show diffuse amyloid first appears in the neocortex up to 20 years before the striatum,[59,60] with a period of rapid amyloid accumulation around 30–40 years of age in DS.[60] Of note, soluble protofibrillar and oligomeric forms of amyloid are elevated before the formation of plaques throughout the brain in DS.[61–64] Similar distributions were observed in various ADAD mutations.[62] These studies are not

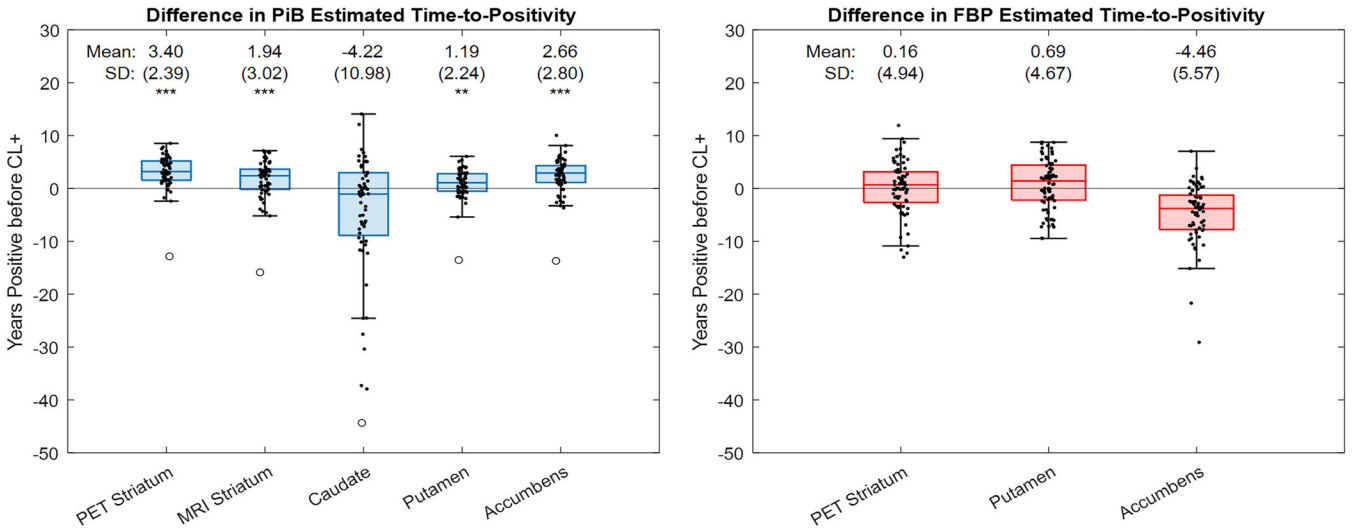

FIGURE 5 Difference in estimated time-to-positivity between the cortex and each striatum-specific ROI. ROIs include the caudate, putamen, accumbens, and a composite MRI-based striatum, all generated using the Harvard Oxford Atlas. Additionally, a PET-generated striatum ROI was created by thresholding the PiB difference image in Figure 3 to +0.75 SUVR. Differences in estimated time-to-positivity relative to the cortex were assessed with a one-tailed paired *t*-test, determining if each region shows earlier estimates than the cortex. PiB (left) shows significantly earlier amyloid positivity in all regions except the caudate. FBP (right) does not show any significant difference with the cortex. A monotonically increasing SILA model could not be created for the caudate and MRI-based striatum ROIs in FBP due to longitudinal variability. One individual in the PiB cohort was deemed an outlier with a *Z*-score < −4 in all ROIs. FBP, [^{18}F]florbetapir; MRI, magnetic resonance image; PET, positron emission tomography; PiB, Pittsburgh Compound-B; ROI, region of interest; SUVR, standardized uptake value ratio.

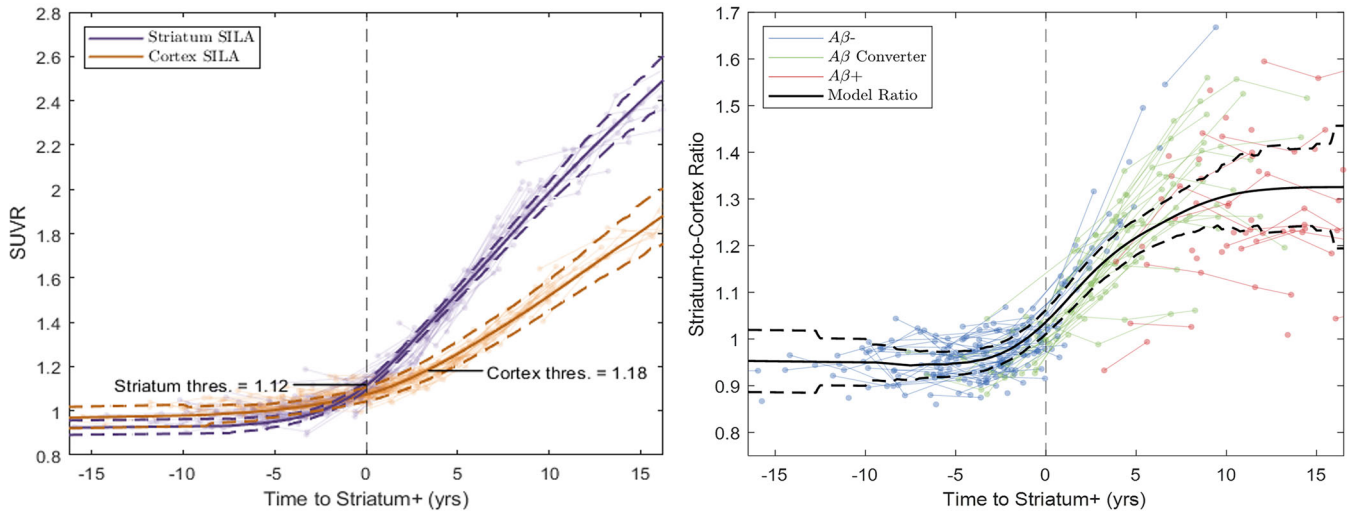

FIGURE 6 SILA models for the cortex and PET-based striatum ROIs of PiB (left). To plot the cortex model along the striatum positivity axis, the cortex model was shifted by the average difference found in Figure 5 (3.40 years). Confidence bands were adjusted accordingly. Participant trajectories for each ROI are displayed as semi-transparent markers. Ratio of the striatum SILA model to the cortex SILA model is displayed right. Participant trajectories are color-coded by cortical amyloid status. All cortically Aβ-converting participants demonstrate earlier striatal positivity. Aβ, beta amyloid; PET, positron emission tomography; PiB, Pittsburgh Compound BROI, region of interest; SILA, sampled iterative local approximation.

specific to the striatum, but the rapid elevated presence of diffuse plaque in the striatum is logically preceded by smaller subunits.[65] PiB binds to oligomeric and larger protofibrillar forms of amyloid, in addition to diffuse plaque (although this binding is weaker when compared to neuritic fibrillar forms).[47,54,55] Significant FBP binding to high molecular weight protofibrils but weaker binding to smaller protofibrils and oligomers is observed.[66,67] *Post mortem* studies with FBP do not comment on binding differences between diffuse plaque and

neuritic plaque scores.[35,56,57,68] These differences between PiB and FBP binding to amyloid subtypes may explain the observed discrepancy in the striatum-first amyloid binding in DS. A direct in vitro comparison of the binding affinities of PiB and FBP to diffuse plaque could clarify this difference.

Eroded WM reference region normalization (i.e., uptake ratio) demonstrates greater longitudinal stability than the WC with FBP. These results are consistent with previous findings that normalization to a high intensity WM reference region increases the power of longitudinal estimates with FBP.[44,45] Additionally, FBP shows significantly higher WM-to-cerebellum ratios than PiB. PET studies in animal models showed that FBP may bind more strongly to myelin than PiB.[69] However in vivo studies suggest that lower relative cortical binding and a smaller dynamic range in FBP may explain the apparent elevated WM binding.[70,71] Therefore, partial volume effects from WM retention may influence the variability of longitudinal measurements in FBP.[72] As the main outcome measure of the current study was the ratio of striatal to cortical signal, partial volume effects are likely minimal.

According to SILA analysis in the PiB cohort, the caudate revealed lower sensitivity to amyloid accumulation and greater variability in estimated time-to-onset than other striatal subregions. Pathological estimates suggest that amyloid plaque develops ubiquitously throughout both the caudate and putamen,[53] so this observation is likely influenced by spatial smoothing or imperfect normalization of atrophied ventricles.[73]

The striatum-specific region that showed the earliest Aβ accumulation was generated by thresholding the PiB difference image between Aβ groups. This region comprised the accumbens, putamen, and inferior ventral caudate. Longitudinal SUVR in this region demonstrated nearly universal early positivity and higher signal in Aβ-converting participants relative to CLs. No sex, age, race, ethnicity, or cognitive status effects were observed. The majority of the DS population in the United States is non-Hispanic White, which may limit the statistical power for evaluating the effects of race and ethnicity in this cohort. A significant interaction between APOE status and tracer is observed, which may be influenced by the difference in age range between the two tracer cohorts. One individual was deemed an outlier in the SILA analysis, as they demonstrated a Z-score < -4 in all ROIs investigated and was amyloid positive in the cortex but not in the striatum for all scans. Interestingly, this participant possesses a mosaic karyotype of DS, meaning only a percentage of their cells exhibit trisomy 21. The impact of mosaicism for trisomy 21 is an active area of study.

There are two main limitations to this work. First, the use of a common template space for image spatial normalization may impact PET estimates for participants with severe structural atrophy (roughly 10% of participants). As mentioned, the striatum-to-cortex outcome measure is likely more robust to atrophy and partial volume effects than SUVR measures alone. Future analyses can be performed using native space regional parcellations to reduce these potential effects. Second, the same longitudinal data used in the creation of the SILA models were also used for the estimates of time-to-positivity. This approach may bias the time-to-positivity estimates in areas of a model with few constituent trajectories. Differences in age and scanning interval between tracer cohorts may additionally bias the results. As the paired t-test used within-participant comparisons, the significance of the time-to-positivity estimates is likely unaffected by these confounds.

Future work should investigate the striatum-first pattern using alternative amyloid radiotracers and other markers of amyloid accumulation as a reference. The speculated binding differences between FBP and PiB may be relevant for all stilbene-based amyloid tracers. One study using stilbene tracer [^{18}F]florbetaben reported moderately elevated striatal uptake in an ADAD cohort.[74] A case study of an individual with early-onset AD also found high florbetaben binding in the striatum.[75] However, these studies were not longitudinal and did not demonstrate the same universal pattern seen with PiB. In particular, a comparison of PiB with other benzothiazole derivatives (e.g., [^{18}F]flutemetamol, [^{18}F]NAV-4694) may clarify the differential sensitivity of this family of radiotracers to striatal accumulation. With the availability of a cyclotron limiting many clinical trial screening sites to F-18 radiotracers, the tracer dependence of striatum-first amyloid accumulation may determine its feasibility as a useful clinical marker. Additionally, fluid biomarkers are actively being analyzed in the ABC-DS study, and these will be investigated as non–PET-derived measures to compare with striatal accumulation.

When comparing amyloid PET tracers PiB and florbetapir, only PiB detects early striatal accumulation in DS, with striatal positivity occurring on average 3.40 years earlier than cortical positivity. These results suggest that the striatum should be used alongside cortical measures as an earlier indicator of amyloid pathology in DS. Understanding the differences in amyloid binding between radiotracers is important for directing upcoming clinical AD trials in DS, for which the assessment of early amyloid burden is a primary treatment target.

ACKNOWLEDGMENTS

Special thanks to the participants and their families who took part in these studies. We also acknowledge the following investigators for their contributions to the ABC-DS study: Ben Handen, PhD (MPI), Brad Christian, PhD (MPI), Elizabeth Head, PhD (MPI), Mark Mapstone, PhD (MPI), Diana Rosas, MD (MGH Site Co-PI), Flo Lai, MD (MGH Site Co-PI), Joe Lee, PhD (Columbia Site Co-PI), Sharon Krinsky-McHale, PhD (Columbia Site Co-PI), Fred Schmitt, PhD (Kentucky Site Co-PI), Jordan Harp, PhD (Kentucky Site Co-PI), Christy Hom, PhD (UCI Site Co-PI), Ira Lott, MD (UCI Site Co-PI), Sigan Hartley, PhD (Wisconsin Site Co-PI), Shahid Zaman, MD PhD (Cambridge Site PI), Beau Ances, MD PhD (Washington University Site PI), Lauren Ptomey, PhD (Kansas University Medical Center Site Co-PI), Jeff Burns, MD (Kansas University Medical Center Site Co-PI), Adam Brickman, PhD (Columbia Core Co-Lead). This work was supported by DS-Connect (The Down Syndrome Registry) and NIH funding U01 AG051406, U01 AG051412, U19 AG068054, P50 AG008702, P30 AG062421, P50 AG016573, P50 AG005133, P50 AG005681, P30 AG062715, P30 AG066519, P30 AG066468, P30 AG072973, P50 HD105353, and U24 AG021886.

CONFLICT OF INTEREST STATEMENT

The authors have no conflicts of interest to disclose. Author disclosures are available in the supporting information.

CONSENT STATEMENT

The study was approved by an Institutional Review Board and conducted in accordance with the Declaration of Helsinki. All participants provided informed consent and assent prior to conducting any study activities.

ORCID

Max McLachlan https://orcid.org/0000-0003-1801-7233

REFERENCES

1. McCarron M, McCallion P, Reilly E, Dunne P, Carroll R, Mulryan N. A prospective 20-year longitudinal follow-up of dementia in persons with Down syndrome. *J Intellect Disabil Res*. 2017;61(9):843-852. doi:10.1111/jir.12390
2. Doran E, Keator D, Head E, et al. Down syndrome, Partial trisomy 21, and absence of Alzheimer's disease: the role of APP. *J Alzheimers Dis JAD*. 2017;56(2):459. doi:10.3233/JAD-160836
3. Mann DMA. The pathological association between down syndrome and Alzheimer disease. *Mech Ageing Dev*. 1988;43(2):99-136. doi:10.1016/0047-6374(88)90041-3
4. Fortea J, Vilaplana E, Carmona-Iragui M, et al. Clinical and biomarker changes of Alzheimer's disease in adults with Down syndrome: a cross-sectional study. *Lancet Lond Engl*. 2020;395(10242):1988. doi:10.1016/S0140-6736(20)30689-9
5. Hithersay R, Startin CM, Hamburg S, et al. Association of Dementia with mortality among adults with Down syndrome older than 35 years. *JAMA Neurol*. 2018;76(2):152. doi:10.1001/jamaneurol.2018.3616
6. Cummings J. Anti-Amyloid Monoclonal antibodies are transformative treatments that redefine Alzheimer's disease therapeutics. *Drugs*. 2023;83(7):569. doi:10.1007/s40265-023-01858-9
7. Sims JR, Zimmer JA, Evans CD, et al. Donanemab in early symptomatic Alzheimer disease: the TRAILBLAZER-ALZ 2 randomized clinical trial. *JAMA*. 2023;330(6):512-527. doi:10.1001/jama.2023.13239
8. van Dyck CH, Swanson CJ, Aisen P, et al. Lecanemab in early Alzheimer's disease. *N Engl J Med*. 2023;388(1):9-21. doi:10.1056/NEJMoa2212948
9. Budd Haeberlein S, Aisen PS, Barkhof F, et al. Two randomized phase 3 studies of aducanumab in early Alzheimer's disease. *J Prev Alzheimers Dis*. 2022;9(2):197-210. doi:10.14283/jpad.2022.30
10. Foley KE, Wilcock DM. Vascular considerations for Amyloid immunotherapy. *Curr Neurol Neurosci Rep*. 2022;22(11):709. doi:10.1007/s11910-022-01235-1
11. Sokol DK, Lahiri DK. Alzheimer's drugs, application for Down syndrome?. *Ageing Res Rev*. 2024;96:102281. doi:10.1016/j.arr.2024.102281
12. Rafii MS, Fortea J. Down Syndrome in a new era for Alzheimer disease. *JAMA*. 2023;330(22):2157. doi:10.1001/jama.2023.22924
13. Strydom A, Coppus A, Blesa R, et al. Alzheimer's disease in Down syndrome: an overlooked population for prevention trials. *Alzheimers Dement Transl Res Clin Interv*. 2018;4:703. doi:10.1016/j.trci.2018.10.006
14. Handen BL, Lott IT, Christian BT, et al. The Alzheimer's biomarker consortium-down syndrome: rationale and methodology. *Alzheimers Dement Diagn Assess Dis Monit*. 2020;12(1):e12065. doi:10.1002/dad2.12065
15. Rafii M, *Alzheimer's Clinical Trial Consortium for Down Syndrome (ACTC-DS) Trial-Ready Cohort—Down Syndrome (TRC-DS)*. clinicaltrials.gov; 2024. Accessed November 9, 2024. https://clinicaltrials.gov/study/NCT04165109
16. Hillerstrom H, Fisher R, Janicki MP, et al. Adapting prescribing criteria for amyloid-targeted antibodies for adults with Down syndrome. *Alzheimers Dement*. 2024;20(5):3649-3656. doi:10.1002/alz.13778
17. Sperling RA, Aisen PS, Beckett LA, et al. Toward defining the preclinical stages of Alzheimer's disease: recommendations from the National Institute on Aging-Alzheimer's Association workgroups on diagnostic guidelines for Alzheimer's disease. *Alzheimers Dement J Alzheimers Assoc*. 2011;7(3):280. doi:10.1016/j.jalz.2011.03.003
18. Rafii MS, Zaman S, Handen BL. Integrating biomarker outcomes into clinical trials for Alzheimer's disease in Down syndrome. *J Prev Alzheimers Dis*. 2021;8(1):48. doi:10.14283/jpad.2020.35
19. Klunk WE, Price JC, Mathis CA, et al. Amyloid deposition begins in the striatum of presenilin-1 mutation carriers from two unrelated pedigrees. *J Neurosci*. 2007;27(23):6174-6184. doi:10.1523/JNEUROSCI.0730-07.2007
20. Gordon BA, Blazey TM, Su Y, et al. Spatial patterns of neuroimaging biomarker change in individuals from families with autosomal dominant Alzheimer disease: a longitudinal study. *Lancet Neurol*. 2018;17(3):241. doi:10.1016/S1474-4422(18)30028-0
21. Koivunen J, Verkkoniemi A, Aalto S, et al. PET amyloid ligand [11C]PIB uptake shows predominantly striatal increase in variant Alzheimer's disease. *Brain*. 2008;131(7):1845-1853. doi:10.1093/brain/awn107
22. Qin Q, Fu L, Wang R, et al. Prominent striatum amyloid retention in early-onset familial Alzheimer's disease with PSEN1 Mutations: a pilot PET/MR study. *Front Aging Neurosci*. 2021;13:732159. doi:10.3389/fnagi.2021.732159
23. Villemagne VL, Ataka S, Mizuno T, et al. High striatal Amyloid β-Peptide deposition across different autosomal Alzheimer disease mutation types. *Arch Neurol*. 2009;66(12):1537-1544. doi:10.1001/archneurol.2009.285
24. Zammit MD, Tudorascu DL, Laymon CM, et al. PET measurement of longitudinal amyloid load identifies the earliest stages of amyloid-beta accumulation during Alzheimer's disease progression in Down syndrome. *NeuroImage*. 2021;228:117728. doi:10.1016/j.neuroimage.2021.117728
25. Lao PJ, Handen BL, Betthauser TJ, et al. Longitudinal changes in amyloid positron emission tomography and volumetric magnetic resonance imaging in the nondemented Down syndrome population. *Alzheimers Dement Diagn Assess Dis Monit*. 2017;9:1. doi:10.1016/j.dadm.2017.05.001
26. Tudorascu DL, Anderson SJ, Minhas DS, et al. Comparison of longitudinal Aβ in non-demented elderly and Down syndrome. *Neurobiol Aging*. 2018;73:171. doi:10.1016/j.neurobiolaging.2018.09.030
27. Cohen AD, McDade E, Christian B, et al. Early striatal Amyloid deposition distinguishes Down syndrome and autosomal dominant AD from late onset amyloid deposition. *Alzheimers Dement J Alzheimers Assoc*. 2018;14(6):743. doi:10.1016/j.jalz.2018.01.002
28. Boerwinkle AH, Gordon BA, Wisch J, et al. Comparison of amyloid burden in individuals with Down syndrome versus autosomal dominant Alzheimer's disease: a cross-sectional study. *Lancet Neurol*. 2023;22(1):55. doi:10.1016/S1474-4422(22)00408-2
29. Zammit MD, Laymon CM, Betthauser TJ, et al. Amyloid accumulation in Down syndrome measured with amyloid load. *Alzheimers Dement Diagn Assess Dis Monit*. 2020;12(1):e12020. doi:10.1002/dad2.12020
30. Klunk WE, Koeppe RA, Price JC, et al. The Centiloid Project: standardizing quantitative amyloid plaque estimation by PET. *Alzheimers Dement J Alzheimers Assoc*. 2014;11(1):1. doi:10.1016/j.jalz.2014.07.003
31. Lao P, Betthauser T, Hillmer A, et al. The effects of normal aging on amyloid-β deposition in nondemented adults with Down syndrome as imaged by [11C]PiB. *Alzheimers Dement J Alzheimers Assoc*. 2016;12(4):380-390. doi:10.1016/j.jalz.2015.05.013
32. Annus T, Wilson LR, Hong YT, et al. The pattern of amyloid accumulation in the brains of adults with Down syndrome. *Alzheimers Dement*. 2016;12(5):538. doi:10.1016/j.jalz.2015.07.490
33. Schöll M, Almkvist O, Axelman K, et al. Glucose metabolism and PIB binding in carriers of a His163Tyr presenilin 1 mutation. *Neurobiol*

Aging. 2011;32(8):1388-1399. doi:10.1016/j.neurobiolaging.2009.08.016
34. Sabbagh MN, Chen K, Rogers J, et al. Florbetapir PET, FDG PET, and MRI in Down syndrome individuals with and without Alzheimer's dementia. *Alzheimers Dement J Alzheimers Assoc*. 2015;11(8):994. doi:10.1016/j.jalz.2015.01.006
35. Fleisher AS, Chen K, Quiroz YT, et al. Florbetapir PET analysis of amyloid-β deposition in the presenilin 1 E280A autosomal dominant Alzheimer's disease kindred: a cross-sectional study. *Lancet Neurol*. 2012;11(12). 10.1016/S1474
36. Sabbagh MN, Fleisher A, Chen K, et al. Positron emission tomography and neuropathologic estimates of fibrillar amyloid-β in a patient with down syndrome and Alzheimer disease. *Arch Neurol*. 2011;68(11):1461-1466. doi:10.1001/archneurol.2011.535
37. Keator DB, Phelan MJ, Taylor L, et al. Down syndrome: distribution of brain amyloid in mild cognitive impairment. *Alzheimers Dement Diagn Assess Dis Monit*. 2020;12(1):e12013. doi:10.1002/dad2.12013
38. Chen CD, McCullough A, Gordon B, et al. Longitudinal head-to-head comparison of 11C-PiB and 18F-florbetapir PET in a Phase 2/3 clinical trial of anti-amyloid-β monoclonal antibodies in dominantly inherited Alzheimer disease. *Eur J Nucl Med Mol Imaging*. 2023;50(9):2669. doi:10.1007/s00259-023-06209-0
39. Keator DB, Doran E, Erp TGMV, et al. [18F]-Florbetapir PET: towards predicting dementia in adults with Down syndrome. Published online February 12, 2018:235440.
40. Keator DB, Doran E, Taylor L, et al. Brain amyloid and the transition to dementia in Down syndrome. *Alzheimers Dement Diagn Assess Dis Monit*. 2020;12(1):e12126. doi:10.1002/dad2.12126
41. Betthauser TJ, Bilgel M, Koscik RL, et al. Multi-method investigation of factors influencing amyloid onset and impairment in three cohorts. *Brain*. 2022;145(11):4065-4079. doi:10.1093/brain/awac213
42. Zammit MD, Betthauser TJ, McVea AK, et al. Characterizing the emergence of amyloid and tau burden in Down syndrome. *Alzheimers Dement*. 2023;20(1):388-398. doi:10.1002/alz.13444
43. Klunk WE, Engler H, Nordberg A, et al. Imaging brain amyloid in Alzheimer's disease with Pittsburgh Compound-B. *Ann Neurol*. 2004;55(3):306-319. doi:10.1002/ana.20009
44. Chen K, Roontiva A, Thiyyagura P, et al. Improved Power for characterizing longitudinal amyloid-β PET changes and evaluating Amyloid-modifying treatments with a cerebral white matter reference region. *J Nucl Med*. 2015;56(4):560-566. doi:10.2967/jnumed.114.149732
45. Landau SM, Fero A, Baker SL, et al. Measurement of longitudinal β-Amyloid change with 18F-Florbetapir PET and standardized uptake value ratios. *J Nucl Med*. 2015;56(4):567-574. doi:10.2967/jnumed.114.148981
46. Royse SK, Minhas DS, Lopresti BJ, et al. Validation of amyloid PET positivity thresholds in centiloids: a multisite PET study approach. *Alzheimers Res Ther*. 2021;13(1):99. doi:10.1186/s13195-021-00836-1
47. Chen CD, Joseph-Mathurin N, Sinha N, et al. Comparing amyloid-β plaque burden with antemortem PiB PET in autosomal dominant and late-onset Alzheimer disease. *Acta Neuropathol (Berl)*. 2021;142(4):689. doi:10.1007/s00401-021-02342-y
48. Lemere CA, Lopera F, Kosik KS, et al. The E280A presenilin 1 Alzheimer mutation produces increased Aβ42 deposition and severe cerebellar pathology. *Nat Med*. 1996;2(10):1146-1150. doi:10.1038/nm1096-1146
49. Ni R, Gillberg PG, Bogdanovic N, et al. Amyloid tracers binding sites in autosomal dominant and sporadic Alzheimer's disease. *Alzheimers Dement*. 2017;13(4):419-430. doi:10.1016/j.jalz.2016.08.006
50. Fukuoka Y, Fujita T, Ito H. Histopathological studies on senile plaques in brains of patients with Down's syndrome. *Kobe J Med Sci*. 1990;36(5-6):153-171.
51. Wisniewski H, VEGIEL J, Popovitch E. Age-associated development of diffuse and thioflavine-S-positive plaques in Down syndrome. *Dev Brain Dysfunct*. 1994;7(6):330-339.
52. Lemere CA, Blusztajn JK, Yamaguchi H, Wisniewski T, Saido TC, Selkoe DJ. Sequence of deposition of heterogeneous Amyloid β-Peptides and APO E in Down syndrome: implications for initial events in amyloid plaque formation. *Neurobiol Dis*. 1996;3(1):16-32. doi:10.1006/nbdi.1996.0003
53. Mann DM, Iwatsubo T. Diffuse plaques in the cerebellum and corpus striatum in Down's syndrome contain amyloid beta protein (A beta) only in the form of A beta 42(43). *Neurodegener J Neurodegener Disord Neuroprotection Neuroregeneration*. 1996;5(2):115-120. doi:10.1006/neur.1996.0017
54. Ikonomovic MD, Buckley CJ, Abrahamson EE, et al. Post-mortem analyses of PiB and flutemetamol in diffuse and cored amyloid-β plaques in Alzheimer's disease. *Acta Neuropathol (Berl)*. 2020;140(4):463. doi:10.1007/s00401-020-02175-1
55. Yamin G, Teplow DB. Pittsburgh Compound-B (PiB) binds amyloid β-protein protofibrils. *J Neurochem*. 2016;140(2):210. doi:10.1111/jnc.13887
56. Choi SR, Schneider JA, Bennett DA, et al. Correlation of amyloid PET ligand florbetapir F 18 (18F-AV-45) binding with β-amyloid aggregation and neuritic plaque deposition in postmortem brain tissue. *Alzheimer Dis Assoc Disord*. 2012;26(1):8. doi:10.1097/WAD.0b013e31821300bc
57. Beach TG, Maarouf CL, Intorcia A, et al. Antemortem-postmortem correlation of florbetapir (18F) PET amyloid imaging with quantitative biochemical measures of Aβ 42 but not Aβ 40. *J Alzheimers Dis*. 2018;61(4):1509-1516. doi:10.3233/JAD-170762
58. Abrahamson EE, Head E, Lott IT, et al. Neuropathological correlates of amyloid PET imaging in Down syndrome. *Dev Neurobiol*. 2019;79(7):750. doi:10.1002/dneu.22713
59. Davidson YS, Robinson A, Prasher VP, Mann DMA. The age of onset and evolution of Braak tangle stage and Thal amyloid pathology of Alzheimer's disease in individuals with Down syndrome. *Acta Neuropathol Commun*. 2018;6:56. doi:10.1186/s40478-018-0559-4
60. Mann DMA. Alzheimer's disease and Down's syndrome. *Histopathology*. 1988;13(2):125-137. doi:10.1111/j.1365-2559.1988.tb02018.x
61. Teller JK, Russo C, Debusk LM, et al. Presence of soluble amyloid β–peptide precedes amyloid plaque formation in Down's syndrome. *Nat Med*. 1996;2(1):93-95. doi:10.1038/nm0196-93
62. Drummond E, Kavanagh T, Pires G, et al. The amyloid plaque proteome in early onset Alzheimer's disease and Down syndrome. *Acta Neuropathol Commun*. 2022;10(1):53. doi:10.1186/s40478-022-01356-1
63. Johannesson M, Sahlin C, Söderberg L, et al. Elevated soluble amyloid beta protofibrils in Down syndrome and Alzheimer's disease. *Mol Cell Neurosci*. 2021;114:103641. doi:10.1016/j.mcn.2021.103641
64. Head E, Helman AM, Powell D, Schmitt FA. Down syndrome, beta-amyloid and neuroimaging. *Free Radic Biol Med*. 2018;114:102-109. doi:10.1016/j.freeradbiomed.2017.09.013
65. Hampel H, Hardy J, Blennow K, et al. The amyloid-β pathway in Alzheimer's disease. *Mol Psychiatry*. 2021;26(10):5481. doi:10.1038/s41380-021-01249-0
66. Conway K, Skovronsky D, Hefti F, 18F-AV-45, an Aβ amyloid PET imaging ligand, binds protofibrillar Aβ aggregates. In: Society of Neuroscience Annual Meeting Abs 141.1/E22.; 2009.
67. Okamura N, Yanai K. Florbetapir (18F), a PET imaging agent that binds to amyloid plaques for the potential detection of Alzheimer's disease. *IDrugs Investig Drugs J*. 2010;13(12):890-899.
68. Sabbagh MN, Fleisher A, Chen K, et al. Positron emission tomography and neuropathologic estimates of fibrillar amyloid-β in a patient With Down Syndrome and Alzheimer disease. *Arch Neurol*. 2011;68(11):1461. doi:10.1001/archneurol.2011.535
69. Auvity S, Tonietto M, Caillé F, et al. Repurposing radiotracers for myelin imaging: a study comparing 18F-florbetaben, 18F-florbetapir, 18F-flutemetamol,11C-MeDAS, and 11C-PiB. *Eur J Nucl Med Mol Imaging*. 2020;47(2):490-501. doi:10.1007/s00259-019-04516-z

70. Su Y, Flores S, Wang G, et al. Comparison of Pittsburgh compound B and florbetapir in cross-sectional and longitudinal studies. *Alzheimers Dement Diagn Assess Dis Monit*. 2019;11:180. doi:10.1016/j.dadm.2018.12.008
71. Landau SM, Thomas BA, Thurfjell L, et al. Amyloid PET imaging in Alzheimer's disease: a comparison of three radiotracers. *Eur J Nucl Med Mol Imaging*. 2014;41(7):1398. doi:10.1007/s00259-014-2753-3
72. Thomas BA, Erlandsson K, Modat M, et al. The importance of appropriate partial volume correction for PET quantification in Alzheimer's disease. *Eur J Nucl Med Mol Imaging*. 2011;38(6):1104-1119. doi:10.1007/s00259-011-1745-9
73. Reig S, Penedo M, Gispert JD, et al. Impact of ventricular enlargement on the measurement of metabolic activity in spatially normalized PET. *NeuroImage*. 2007;35(2):748-758. doi:10.1016/j.neuroimage.2006.12.015
74. Sala-Llonch R, Falgàs N, Bosch B, et al. Regional patterns of 18F-florbetaben uptake in presenilin 1 mutation carriers. *Neurobiol Aging*. 2019;81:1-8. doi:10.1016/j.neurobiolaging.2019.04.010
75. Um YH, Choi WH, Jung WS, Park YH, Lee CU, Lim HK. A Case Report of a 37-Year-Old Alzheimer's disease patient with prominent striatum amyloid retention. *Psychiatry Investig*. 2017;14(4):521. doi:10.4306/pi.2017.14.4.521

SUPPORTING INFORMATION

Additional supporting information can be found online in the Supporting Information section at the end of this article.

How to cite this article: McLachlan M, Bettcher B, McVea A, et al. The striatum is an early, accurate indicator of amyloid burden using [^{11}C]PiB in Down syndrome: Comparison of two radiotracers. *Alzheimer's Dement*. 2025;21:e70141. https://doi.org/10.1002/alz.70141